Internet Appendix

Comparing the risk spillover from oil and gas to investment grade and high-yield bonds through optimal copulas

Appendix A: Recent trends in international oil and gas industry

Global oil markets have been experiencing a period of extraordinary changes in the recent years which can mainly be attributed to (i) the imposition of sanctions and crude oil production restraint on key producing countries (for example, Iran and Venezuela) and (ii) oil demand growth shifting towards Asia. These changes are expected to have profound impact on international trade and other asset markets. With regard to oil supply growth, in 2018, total liquid production increased by 2.2 million barrel per day (mb/d) (IEA, 2019a). While the US is the major contributor (about 70%) to this growth, other important suppliers are Brazil, Canada, Norway and Guyana. As a consequence of its shale revolution, the US is a dominant oil exporter and it will become a net oil exporter in 2021. This change has important implications. The crude oil importers (particularly in Asia) now have greater choice of suppliers that leads to higher operational and trading flexibility, and reduced dependence on oil-rich Middle Eastern countries. This phenomenon ultimately brings greater oil security around the world. Although oil demand has been growing in recent years, the growth was harmed due to weak economic outlook in many countries, continuing trade disagreement between the US and China, and disorderly Brexit. Nonetheless, the oil demand growth is underpinned by increased oil demand in developing countries, particularly in China and India. About 44% (7.1 mb/d) of the global demand growth is expected to be accounted by these two countries. Increase in oil demand is also coming from increased demand for plastics and petrochemicals. These two sectors contribute to about 30% of the global oil demand growth. Another major contributor to oil demand growth is the expansion in the aviation sector.

The demand for natural gas increased by 4.6% in 2018 and this rate is the highest since 2010. About 45% of the total increase in global energy consumption is accounted by natural gas (IEA, 2019b). The increase in demand mainly comes from the USA and China

due to their economic growth, a move from coal to gas and high weather-related energy needs. Other contributors to this growth are Middle Eastern and North African countries. The Chinese government's goal to improve air quality, and Middle Eastern and North African countries' abundant domestic resources are encouraging the use of natural gas in industrial application. Nonetheless, this growth is not expected to sustain in future as power generation is the main use of natural gas which is facing increased competition from renewable energy. With regard to supply growth, the USA is the largest supplier that experienced a 11.5% growth in gas production in 2018. This growth is primarily attributable to wet and dry shale gas resources. Other major gas suppliers are China, Australia, Russia, and Iran. While the global gas trade is largely driven by liquefied natural gas (LNG), larger investment in this sector is necessary to avoid shrinking capacity margin. While difference in regional (particularly between Asia and Europe) prices was a main characteristic of the global gas market, this difference has decreased sharply towards the end of 2018. This change can be attributed to well-supplied markets and the expansion of LNG trade. Further, several governments (for example China, India and Pakistan) have revised prices in domestic market for a greater convergence to the global gas market.

The major regulatory challenge faced by the global energy sector is the 2020 International Maritime Organization (IMO) regulation change. IMO takes a strategy to reduce carbon emission by at least 50% by 2050. This regulation can have a far-reaching impact on the energy sector as energy shipping and refining industries have to comply with certain standard. It is expected that some non-compliance in the initial stage will make the market tight.

Apart from the regulatory challenge, the fundamental challenge of the energy sector is its intrinsic volatility. The oil and gas producers need to develop a resilient strategy to face major uncertainties associated with (i) an over- or under-supplied market, and (ii)

transformation from fossil fuels to renewable energy sources. Oil and gas companies typically focus on maintaining a lower break-even price, having adequate capital and innovation of new technologies to face these uncertainties. For instance, Shell has divested its oil sand business in Athabasca in May 2017, and in 2018, BP has announced that new project will be approved only if it is profitable at less than $40 per barrel. Both of these examples aim to reduce break-even prices. Overall, the world will continue to depend on oil and gas, and demand, supply and resulting price volatility is likely to persist in the market. Therefore, operators and investors in the oil and gas market need plan of action particularly with regard to portfolio resilience, innovation and capital efficiency.

Appendix B: Time varying optimal copula (TVOC) modelling

The optimal copula (OC) modelling involves five algorithmic steps:

Step 1: We use a two-step semiparametric method namely the canonical maximum likelihood method to estimate copula parameters (Cherubini et al., 2004; Aloui et al., 2013). Since the presence of conditional heteroskedasticity is a common feature of financial returns, we use the following VARX-GARCH (1, 1) model with skewed-t distribution to filter the return series and derive standardized residuals.

$$r_t = \mu_t + \varepsilon_t \quad \text{(A.1)}$$

$$\mu_t = C_0 + C_1\mu_{t-1} + A_0 x_t \quad \text{(A.2)}$$

$$\sigma_t^2 = \omega + \alpha\varepsilon_{t-1}^2 + \beta\sigma_{t-1}^2 \quad \text{(A.3)}$$

where r_t denotes the log return of high-yield (HY) or investment grade (IG) bond index at time t. The mean equation μ_t is modeled by the vector autoregression process with exogenous variables: oil and gas returns. Note that the GARCH parameters take non-negative values ($\omega > 0$, $\alpha \geq 0$, $\beta \geq 0$) in order to guarantee the positivity of σ_t^2. The skewed-t distribution is used as the energy and bond return series exhibit fat-tails and skewed behavior (see Table 1).[1] Uddin et al. (2018) argue that skewed-t distribution is particularly suitable for modelling return distributions with fat tails.[2] The marginal distribution is estimated based on the empirical distribution function of corresponding standardized residuals as

$$\hat{F}_{\epsilon i}(\varepsilon) = \frac{1}{T+1}\sum_{t=1}^{T} I_{(\hat{\varepsilon}_{i,t} \leq \varepsilon)} \quad \text{(A.4)}$$

[1] Following Hansen (1994), skewed-t's density distribution can be defined as:

$$f(z_t, v, \eta) = \begin{cases} bc\left(1 + \frac{1}{v-2}\left(\frac{bz_t+a}{1-\eta}\right)^2\right)^{-(v+1)/2}, & z_t < -a/b \\ bc\left(1 + \frac{1}{v-2}\left(\frac{bz_t+a}{1-\eta}\right)^2\right)^{-(v+1)/2}, & z_t \geq -a/b \end{cases}$$

where, v is the degree of freedom parameters ($2 < v < \infty$) and η is the symmetric parameter ($-1 < \eta < 1$). The constants *a*, *b*, and *c* are $a = 4\eta c\left(\frac{v-2}{v-1}\right)$, $b^2 = 1 - 3\eta - a^2$, and $c = \frac{\Gamma\left(\frac{v+1}{2}\right)}{\sqrt{\pi(v-2)}\,\Gamma\left(\frac{v}{2}\right)}$

[2] The best marginal model is selected, firstly by considering different combinations of the lag parameters, and secondly, by choosing the optimal lag structure of the parameters based on the minimum value of Akaike Information Criterion (AIC).

where $I_{(.)}$ is an indicator function which takes a value of 1 if $\hat{\varepsilon}_{i,t} \leq \varepsilon$, and 0, if otherwise. Through estimating the marginal distribution, the return series $\{r_{i,t}\}_{t=1}^{T}$ is transformed in to uniform (0,1) distribution series $\{\hat{F}_{\varepsilon i}(\hat{\varepsilon}_{i,t})\}_{t=1}^{T}$ and copula parameter θ is estimated via maximum pseudo-likelihood in the following manner:

$$\hat{\theta}_{i,j} = \text{argmax}_{\theta} \sum_{t=1}^{T} \ln C_{ij}\left(\hat{F}_{\varepsilon X}(\hat{\varepsilon}_{X,t}), \hat{F}_{\varepsilon Y}(\hat{\varepsilon}_{Y,t}); \theta\right) \quad \text{(A.5)}$$

where i and j respectively include the original and rotated copula functions. The details of copula functions and their specifications are provided in Appendix Table A.1.

Step 2: Since dependence across markets can be complex and non-linear (positive dependence and negative dependence), Kendall's τ is used to measure the direction and intensity of the relationship. Covariance based correlation is not preserved by copula whereas Kendall's τ is a constant of the copula. That is, any correlated variates with the same copula will have the τ of that copula. In this step, Kendall's τ is computed for the subsample of time point t and it is denoted by τ_t. This step enables to measure the cross-market nonlinear and asymmetric negative dependence using proper copulas.[3]

Step 3: In order to select OC for the bond and energy returns, we need to first ascertain their dependence relationship by statistical inference. To this vein, we test the following hypotheses:

Hypothesis 1: Null hypothesis $H_0 : \tau = 0$; Alternate hypothesis $H_1 : \tau < 0$. This hypothesis involves one-sided lower tail dependence.

[3] In the case of random variables *X* and *Y* with copula *C*, Kendall's τ is estimated as:
$\tau(\hat{\theta}) = 4\int_0^1 \int_0^1 C(u,v;\hat{\theta}) dC(u,v;\hat{\theta}) - 1$. In simple word $\tau(\hat{\theta}) = 4\text{E}[\text{C(u, v)}] - 1$ where E[] is the expectation operator, which is the key, and the 4 and -1 are simply for interpretation purposes.
In the presence of the second order mixed partial derivative of the copula, $C(u,v;\hat{\theta})$, and $dC(u,v;\hat{\theta}) = c(u,v;\hat{\theta})dudv$, Kendall's τ is

$$\tau(\hat{\theta}) = 4\int_0^1 \int_0^1 C(u,v;\hat{\theta}) c(u,v;\hat{\theta}) dudv - 1$$

If Clayton characterizes the copula-dependence structure, then $\tau(\hat{\theta}) = \frac{\hat{\theta}}{\hat{\theta}+2}, \hat{\theta} \in (0,\infty)$ while if Gumbel characterizes the copula-dependence structure, then $\tau(\hat{\theta}) = \frac{\hat{\theta}-1}{\hat{\theta}}, \hat{\theta} \in (1,\infty)$

Hypothesis 2: Null hypothesis $H_0 : \tau = 0$; Alternate hypothesis $H_1 : \tau > 0$. This hypothesis involves one-sided upper tail dependence.

Given the significance level α, if $K^* < -u_\alpha$, it indicates a significant negative dependence between the two series and the rejection of hypothesis 1.[4] In such case, the OC of time point *t* is selected from the copula family {Normal, t, R_1 Clayton, R_2 Clayton, R_1 Gumbel, R_2 Gumbel} on the basis of a comparison of their log-likelihood values; otherwise, we move to step 4.

Step 4: If $K^* > u_\alpha$, it is indicative of a significant positive dependence between the series and the rejection of hypothesis 2. In this case, the OC of time point t is selected from the copula family {Normal, t, Clayton, Gumbel, R Clayton, R Gumbel}; otherwise, we move to step 5.

Step 5: If the observations are found to be statistically independent and we fail to reject any of the hypothesis, the OC of time point t is selected from the copula family {Normal, t, Clayton, Gumbel, R Clayton, R Gumbel, R_1 Clayton, R_1 Gumbel, R_2 Clayton, R_2 Gumbel}.[5]

[4] The test statistic is $K^* = \frac{K - E_0(K)}{\sqrt{Var_0(K)}} = \frac{K}{\sqrt{Var_0(K)}} = \frac{\binom{n}{2}.\hat{\tau}}{(n(n-1)(2n+5)/18)^{1/2}} \xrightarrow{d} N(0,1)$ (Hollander & Wolfe, 1973).

[5] R represents the original bivariate copula density function (either Clayton or Gumbel) rotating 180 degrees through symmetric axis of $\begin{cases} u = 0.5 \\ v = 0.5 \end{cases}$. R_1 and R_2 respectively represents the original bivariate copula density function (either Clayton or Gumbel) accomplishing mirrored transformation through the symmetric plane of $u = 0.5$ and $v = 0.5$. So, *R*, R_1 and R_2 respectively indicate bivariate copula density function rotating 180, 90, and 270 degrees.

Table A.1 Copula functions

Copula name	Formula	Parameter	Distribution	Dependence	Tail Dependence
Normal	$C_N(u,v,\rho) = \theta(\theta^{-1}(u), \theta^{-1}(v))$	$\rho \in [-1\ 1]$	Symmetric	P.D/ N.D	No
Student-t	$C_{ST}(u,v,\rho,\pi) = T(t_\pi{}^{-1}(u), t_\pi{}^{-1}(v))$	$\rho \in [-1\ 1]$	Symmetric	P.D/ N.D	All
Clayton	$C_C(u,v:\theta) = max\left\{\left(u^{-\theta} + v^{-\theta} - 1\right)^{-1/\theta}, 0\right\}$	$\theta \in [-1,\infty)\backslash\{0\}]$	Asymmetric	P.D	Lower – Lower
R1 (90^0 Rotated) Clayton	$C_{R_1C}(u,v:\theta) = v - \left((1-u)^{-\theta} + v^{-\theta} - 1\right)^{-\frac{1}{\theta}}$	$\theta \in [-1,\infty)\backslash\{0\}]$	Asymmetric	N.D	Upper – Lower
R (180^0 Rotated) Clayton	$C_{RC}(u,v:\theta) = u + v - 1 + C_C(1-u, 1-v;\theta)$	$\theta \in [-1,\infty)\backslash\{0\}]$	Asymmetric	P.D	Upper – Upper
R2 (270^0 Rotated) Clayton	$C_{R_2C}(u,v:\theta) = u - \left(u^{-\theta} + (1-v)^{-\theta} - 1\right)^{-\frac{1}{\theta}}$	$\theta \in [-1,\infty)\backslash\{0\}]$	Asymmetric	N.D	Lower – Upper
Gumbel	$C_G(u,v:\theta) = exp(-((-log\,u)^\theta + (-log\,v)^\theta)^{1/\theta}$	$\theta \in [1,\infty)$	Asymmetric	P.D	Upper – Upper
R1 (90^0 Rotated) Gumbel	$C_{RG}(u,v:\theta) = v - C_G(1-u, v;\theta)$	$\theta \in [1,\infty)$	Asymmetric	N.D	Lower – Upper
R (180^0 Rotated) Gumbel	$C_{RG}(u,v:\theta) = u + v - 1 + C_G(1-u, 1-v;\theta)$	$\theta \in [1,\infty)$	Asymmetric	P.D	Lower – Lower
R2 (270^0 Rotated) Gumbel	$C_{RG}(u,v:\theta) = u - C_G(u, 1-v;\theta)$	$\theta \in [1,\infty)$	Asymmetric	N.D	Upper – Lower

Notes: P.D and N.D are positive average dependence and negative average dependence. In the case of normal copula, $\theta^{-1}(u)$ and $\theta^{-1}(v)$ represent standard normal quantile functions, θ denotes bivariate standard normal cumulative distribution function, ρ is the correlation between the functions. With regard to student-t copula, $t_\pi{}^{-1}(u)$ and $t_\pi{}^{-1}(v)$ indicate quantile functions of the univariate student-t distribution, T denotes the bivariate student-t cumulative distribution, u and v are degree-of-freedom parameter and ρ is the correlation between the functions. Bivariate normal copula and student-t copula belong to symmetric copula family. While normal copula does not capture tail dependence, student-t copula captures equal lower and upper tail dependence. Asymmetric copula family includes Clayton copula, Rotated Clayton copula, Gumbel copula, and Rotated Gumbel copula. Clayton, 180^0 Rotated Clayton, Gumbel and 180^0 Rotated Gumbel copulas measure asymmetric positive dependence. That is, they measure two positive cases when both the bond and energy markets are either bullish or bearish. While Clayton copula and 180^0 Rotated Gumbel copula can only capture lower tail dependence, Gumbel copula and 180^0 Rotated Clayton copula can only capture upper tail dependence. 90^0 and 270^0 Rotated Clayton and 90^0 and 270^0 Rotated Gumbel copulas capture negative dependence. They capture a lower-upper tail and upper-lower tail dependence. Therefore, they measure two negative cases, when one market (such as bond) is bullish and other market (such as energy) is bearish.

Table A.2 The log-likelihood values for different copula models

	TVOC	TVP-Normal	TVP-t	Normal	Student-t
S&P HY – Oil	59.15	18.52	19.56	8.65	9.22
S&P IG – Oil	46.24	5.76	7.99	1.43	3.11
EN HY – Oil	54.81	10.61	20.06	2.54	1.08
EN IG – Oil	44.31	8.49	10.54	1.25	9.45
S&P HY – Gas	38.58	10.71	12.21	3.54	10.01
S&P IG – Gas	19.51	5.16	19.35	6.24	6.15
EN HY – Gas	37.29	10.80	21.39	6.76	7.54
EN IG – Gas	19.22	6.17	9.19	0.88	2.56

Note: This table compares the log-likelihood values of time-varying optimal copula (TVOC) with time-varying parameter (TVP) copulas (TVP-Normal and TVP-t) and non-dynamic or static copulas (Normal and Student-t). S&P IG, S&P HY, EN IG, and EN HY respectively indicate daily returns of S&P500 investment grade corporate bond index, S&P U.S high-yield corporate bond index, S&P500 investment grade energy corporate bond index, and S&P U.S. high-yield energy corporate bond index. Oil and gas respectively represent oil and gas futures returns. For assuring comparability, the log-likelihood value of the TVOC model is defined as: $L = \frac{\sum_{t=1}^{T-w+1} l_t}{T-w+1} . \frac{T}{w}$, where l_t is the best-fitting copula log-likelihood value at time point *t*, *w* is the length of the rolling window and T is the length of the series.

Table A.3: Loglikelihood ratios of volatility models with different distribution assumptions

		$R_t^{S\&P\ IG}$	$R_t^{S\&P\ HY}$	$R_t^{EN\ IG}$	$R_t^{EN\ HY}$	R_t^{Oil}	R_t^{Gas}
GARCH (1,1)	NORM	-216.50	1546.07	-657.30	705.63	-5515.67	-6504.45
	SNORM	-216.98	1545.85	-657.83	705.46	-5522.89	-6505.13
	STD	-217.80	1534.48	-657.97	688.03	-5532.82	-6505.61
	SSTD	**-215.15**	**1555.37**	**-650.86**	**708.83**	-5516.37	**-6495.45**
	GED	-221.26	1543.17	-651.50	705.63	-5522.48	-6506.22
	SGED	-221.76	1543.01	-651.89	705.46	**-5514.26**	-6506.95
EGARCH (1,1)	NORM	-224.47	1540.14	-664.29	700.83	-5518.30	-6508.79
	SNORM	-222.55	1530.16	-662.09	688.02	-5539.58	-6507.37
	STD	-215.91	1555.29	-650.98	708.86	-5515.75	-6496.14
	SSTD	-219.72	1542.92	-660.23	700.83	-6620.03	-7708.66
	GED	-218.89	1553.02	-652.92	704.83	-5511.01	-6497.86
	SGED	-216.62	1543.42	-651.12	691.76	-5530.52	-6497.52
GJR-GARCH (1,1)	NORM	-219.21	1553.11	-654.39	708.35	-5522.78	-6498.87
	SNORM	-219.98	1553.03	-654.48	708.33	-5523.94	-6499.63
	STD	-222.94	1550.78	-656.38	704.30	-5520.06	-6501.12
	SSTD	-220.65	1539.94	-654.65	691.22	-5539.43	-6500.90
	GED	-240.74	1490.09	-682.44	620.47	-5568.24	-6558.56
	SGED	-241.19	1487.14	-684.16	618.55	-5568.60	-6559.05
APARCH (1,1)	NORM	-244.42	1481.19	-687.58	609.87	-5558.84	-6564.61
	SNORM	-242.48	1470.56	-684.41	592.24	-5595.36	-6559.17
	STD	-245.74	1485.14	-687.75	619.92	-5582.20	-6567.06
	SSTD	-246.22	1482.76	-688.95	618.09	-5582.20	-6567.75
	GED	-249.40	1476.57	-692.41	609.14	-5573.90	-6572.30
	SGED	-247.48	1462.67	-689.34	590.80	-5610.26	-6567.76

Note: Bold numbers indicate best-fitted model with the highest loglikelihood values. NORM: Normal distribution; SNORM: Skewed normal distribution; STD: Student-t distribution; SSTD: Skewed Student-t distribution; GED: Generalized error distribution; SGED: Skewed generalized error distribution. See notes to Table A.2 for further details.

Table A.4 Conditional coverage Backtesting tests: Downside VaR

	S&P IG	S&P HY	EN IG	EN HY	Oil	Gas
DB_1	6.140	0.521	6.335	1.263	6.529	0.192
	(0.046)	(0.771)	(0.042)	(0.532)	(0.038)	(0.909)
DB_2	2.492	3.423	2.387	2.890	9.196	0.193
	(0.359)	(0.242)	(0.198)	(0.308)	(0.027)	(0.979)
DB_3	5.339	3.861	2.175	2.929	9.283	1.609
	(0.340)	(0.428)	(0.161)	(0.629)	(0.054)	(0.807)
DB_4	5.245	4.002	2.198	3.034	8.962	1.832
	(0.294)	(0.513)	(0.322)	(0.743)	(0.111)	(0.872)
DB_5	2.516	4.972	3.321	2.331	10.602	0.524
	(0.390)	(0.018)	(0.298)	(0.533)	(0.031)	(0.971)
DB_6	2.463	4.394	3.024	2.831	13.906	2.397
	(0.290)	(0.133)	(0.280)	(0.802)	(0.016)	(0.792)
DB_7	6.142	2.154	4.927	3.052	10.538	0.323
	(0.105)	(0.541)	(0.348)	(0.384)	(0.015)	(0.956)
DQ_1	3.053	4.119	3.773	4.050	0.555	0.219
	(0.217)	(0.128)	(0.152)	(0.132)	(0.758)	(0.896)
DQ_2	3.660	5.057	4.119	4.835	0.693	0.226
	(0.160)	(0.080)	(0.128)	(0.589)	(0.707)	(0.893)
DQ_3	8.415	7.858	6.104	5.976	2.446	0.886
	(0.038)	(0.049)	(0.107)	(0.113)	(0.485)	(0.829)
$DQVaR_1$	9.046	12.045	6.267	4.442	3.314	1.536
	(0.060)	(0.017)	(0.180)	(0.510)	(0.507)	(0.820)
$DQVaR_2$	3.664	5.637	5.465	4.935	4.347	0.361
	(0.300)	(0.131)	(0.141)	(0.740)	(0.226)	(0.948)
$DQVaR_3$	8.562	9.013	7.809	7.941	6.444	0.996
	(0.128)	(0.109)	(0.167)	(0.160)	(0.265)	(0.963)
LR	9.349	15.111	8.974	11.042	10.851	1.971
	(0.229)	(0.035)	(0.255)	(0.137)	(0.145)	(0.961)

Note: The entries are the estimated VaRs and corresponding p-values (in the parentheses). Thirteen conditional coverage tests are used. Among the tests, seven are based on the dynamic binary regression model (DB) proposed by Dumitrescu et al. (2012) where explanatory variables are lagged VaRs and lagged violations specifications; six tests are based on the dynamic quantile tests (DQ) of Engle and Manganelli (2004) that include several lags of violations variable and VaR; and one test is the Markov Chain based LR test of Christoffersen (1998). See notes to Table A.2 for further details.

Table A.5 Conditional coverage Backtesting tests: Upside VaR

	S&P IG	S&P HY	EN IG	EN HY	Oil	Gas
DB_1	0.416	0.997	0.416	7.152	0.104	0.123
	(0.812)	(0.607)	(0.812)	(0.028)	(0.949)	(0.941)
DB_2	2.184	1.259	8.526	15.505	0.884	4.977
	(0.535)	(0.739)	(0.036)	(0.001)	(0.829)	(0.173)
DB_3	2.512	4.325	1.868	17.347	3.120	5.102
	(0.642)	(0.364)	(0.760)	(0.002)	(0.538)	(0.277)
DB_4	5.534	5.215	1.878	17.406	3.797	4.203
	(0.354)	(0.390)	(0.866)	(0.004)	(0.579)	(0.521)
DB_5	2.218	1.514	10.088	16.058	2.739	5.343
	(0.696)	(0.824)	(0.039)	(0.003)	(0.602)	(0.254)
DB_6	2.220	1.546	10.280	17.130	2.555	0.909
	(0.818)	(0.908)	(0.068)	(0.004)	(0.768)	(0.970)
DB_7	0.426	1.272	0.420	9.625	2.049	0.640
	(0.935)	(0.736)	(0.936)	(0.022)	(0.562)	(0.887)
DQ_1	2.403	1.010	0.641	1.842	0.710	1.340
	(0.301)	(0.604)	(0.726)	(0.398)	(0.701)	(0.512)
DQ_2	2.156	0.994	0.634	1.611	0.777	1.154
	(0.340)	(0.608)	(0.728)	(0.447)	(0.678)	(0.561)
DQ_3	2.201	1.107	1.537	4.282	0.909	4.251
	(0.532)	(0.775)	(0.674)	(0.233)	(0.823)	(0.236)
$DQVaR_1$	2.267	1.222	1.859	5.059	1.034	4.616
	(0.687)	(0.874)	(0.762)	(0.281)	(0.905)	(0.329)
$DQVaR_2$	2.162	1.302	0.635	3.723	2.749	1.711
	(0.539)	(0.729)	(0.888)	(0.293)	(0.432)	(0.634)
$DQVaR_3$	2.404	1.458	1.677	6.192	13.583	4.767
	(0.791)	(0.918)	(0.892)	(0.288)	(0.018)	(0.445)
LR	4.292	1.580	2.063	7.056	13.874	5.937
	(0.746)	(0.979)	(0.956)	(0.423)	(0.053)	(0.547)

Note: See notes to Table A.2 and Table A.4.

Figure A.1 Time trend of bond indices and energy prices

Panel A: Time trend of bond indices

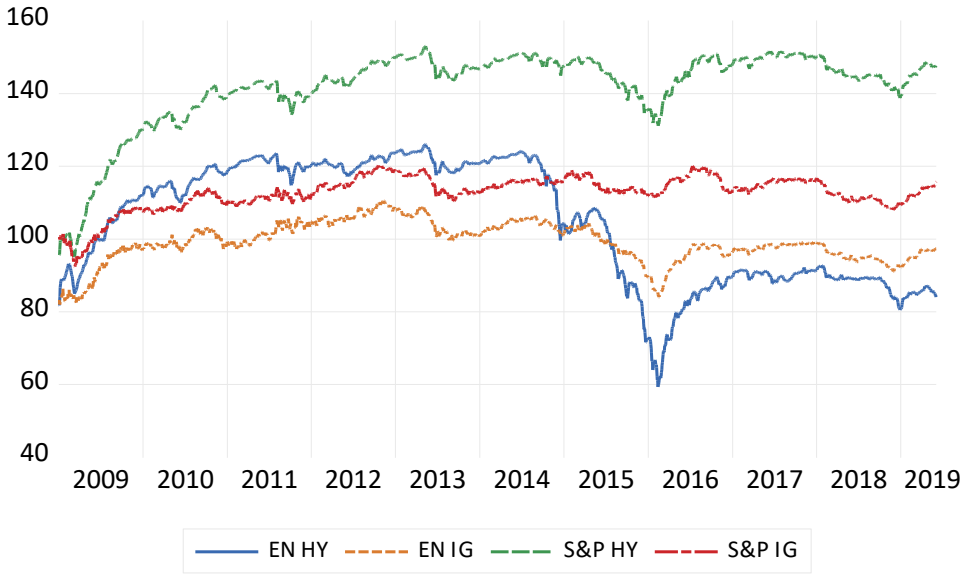

Panel B: Time trend of energy prices

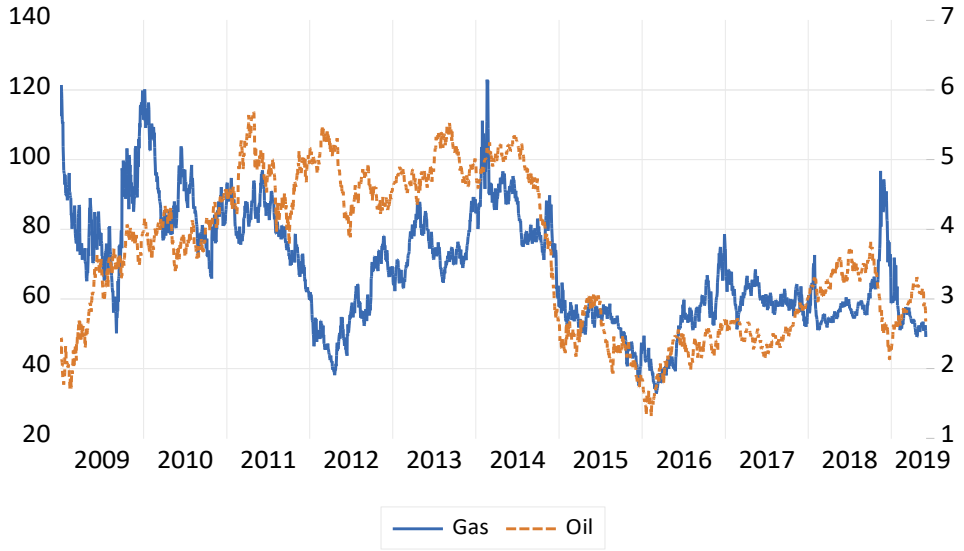

Notes: In Panel B, oil and gas futures prices are respectively in the right and left axis. See notes to Table A.2 for further details. Source: Authors' own estimation.

Figure A.2 Time varying optimal copula estimates for oil and bond returns

Panel A: Time varying optimal copula estimates for the oil and EN HY returns

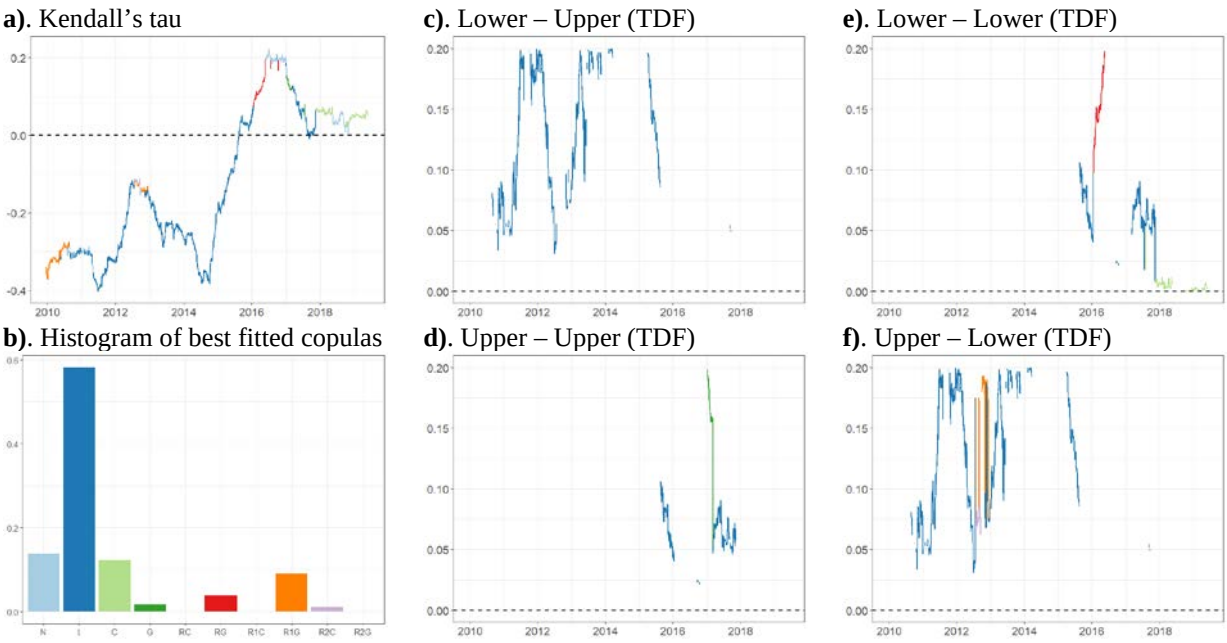

Panel B: Time varying optimal copula estimates for the oil and EN IG returns

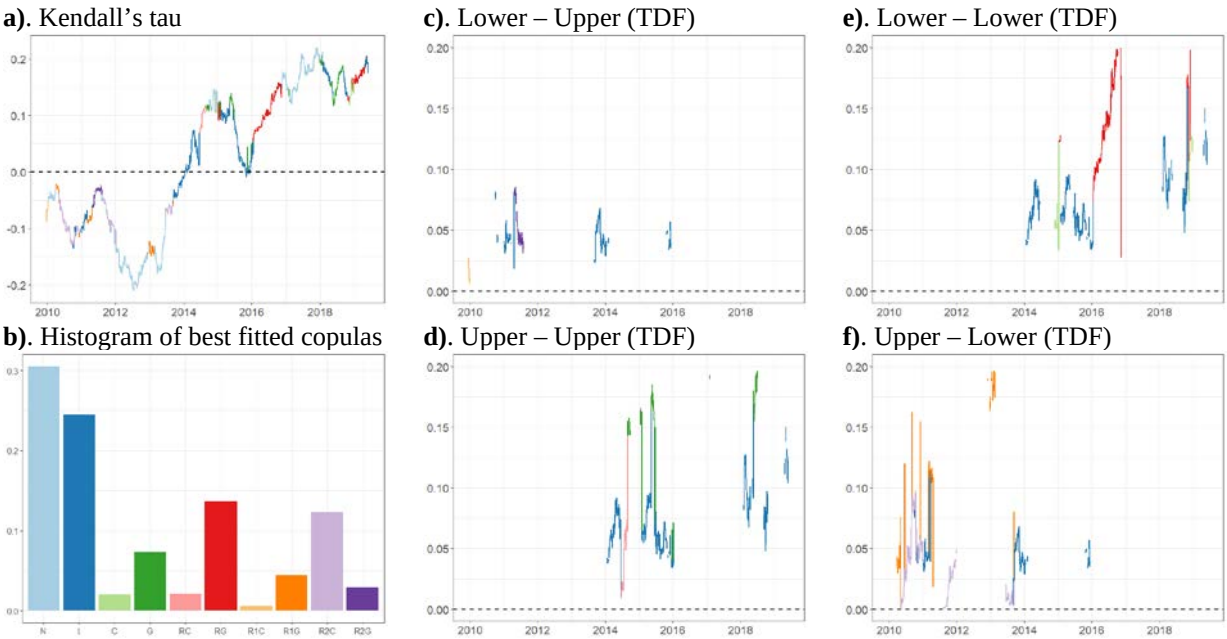

Note: In each Panel, (a) shows the Kendal's tau derived from the tail dependence parameters and (b) displays the percentages of best-fitted copula. N: normal; t: student-t; C: Clayton; G: Gumbel; RC: 180° Rotated Clayton; RG: 180° Rotated Gumbel; R1C: 90° Rotated Clayton; R1G: 90° Rotated Gumbel; R2C: 270° Rotated Clayton; R2G: 270° Rotated Gumbel. (c)-(f) present the time-varying tail dependence parameters. TDF stands for tail-dependence function. See notes to Table A.2 for further details. Source: Authors' own estimation.

Figure A.3 Time varying optimal copula estimates for gas and bond returns

Panel A: Time varying optimal copula estimates for the gas and EN HY returns

a). Kendall's tau

c). Lower – Upper (TDF)

e). Lower – Lower (TDF)

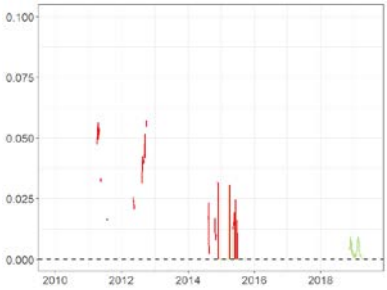

b). Histogram of best fitted copulas

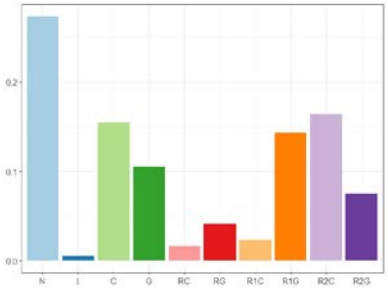

d). Upper – Upper (TDF)

f). Upper – Lower (TDF)

Panel B: Time varying optimal copula estimates for the gas and EN IG returns

a). Kendall's tau

c). Lower – Upper (TDF)

e). Lower – Lower (TDF)

b). Histogram of best fitted copulas

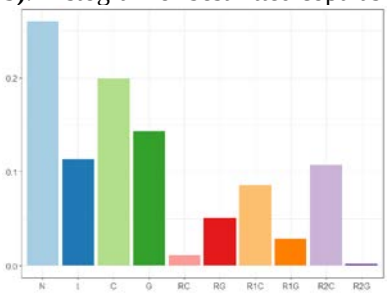

d). Upper – Upper (TDF)

f). Upper – Lower (TDF)

Note: See notes to Figure A.2 and Table A.2.

Figure A.4 Downside and upside VaR, CoVaR and ΔCoVaR

Panel A: Downside and upside VaR and CoVaR

i). From oil to EN HY bond

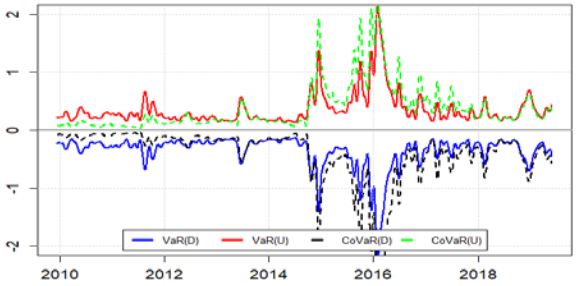

ii). From oil to EN IG bond

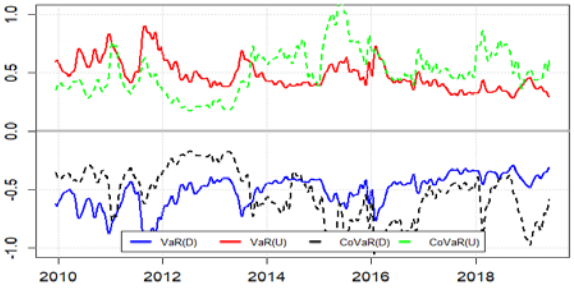

iii). From gas to EN HY bond

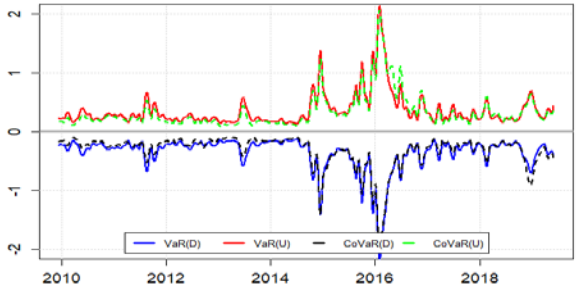

iv). From gas to EN IG bond

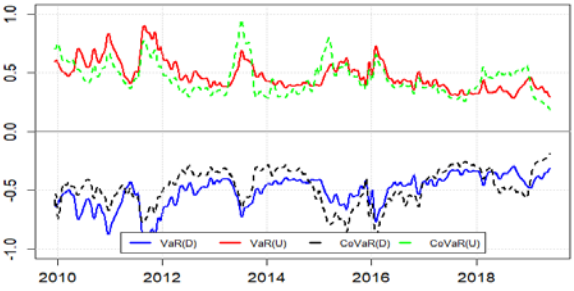

Panel B: Downside and upside ΔCoVaR from energy to bond returns

i). From oil to EN HY bond

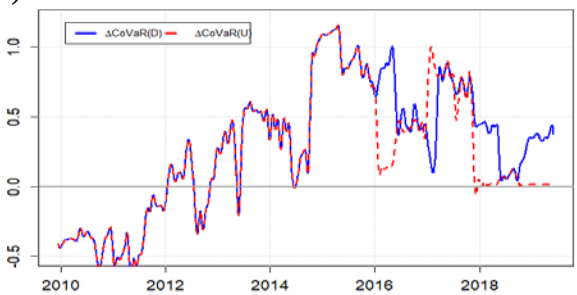

ii). From oil to EN IG bond

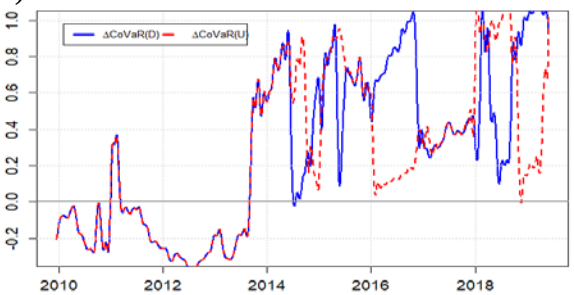

iii). From gas to EN HY bond

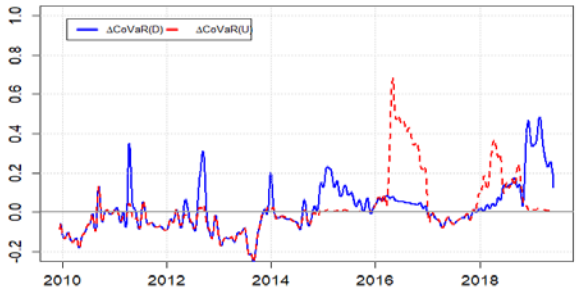

iv). From gas to EN IG bond

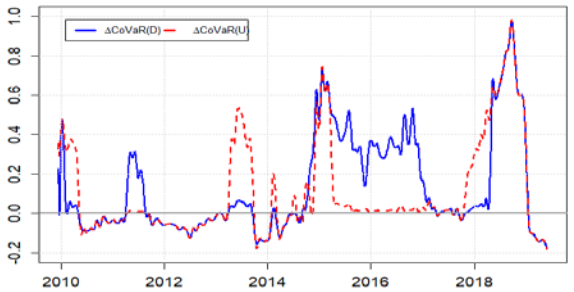

Notes: VaR(D), CoVaR(D) and ΔCoVaR (D) are the downside value-at-risk and conditional VaR and delta CoVaR. VaR(U), CoVaR(U), and ΔCoVaR (U) are the upside VaR, conditional VaR, and delta CoVaR. Downside and upside VaRs and CoVaRs are calculated under the quantiles of 5% and 95%, respectively. See notes to Table A.2 for further details.

Figure A.5 Histogram of VaRs

Panel A: Overall market index

a). Downside VaR

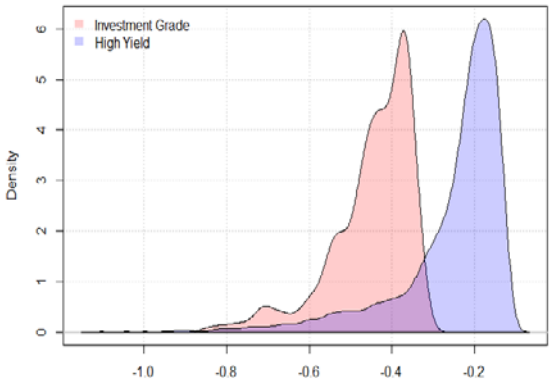

b). Upside VaR

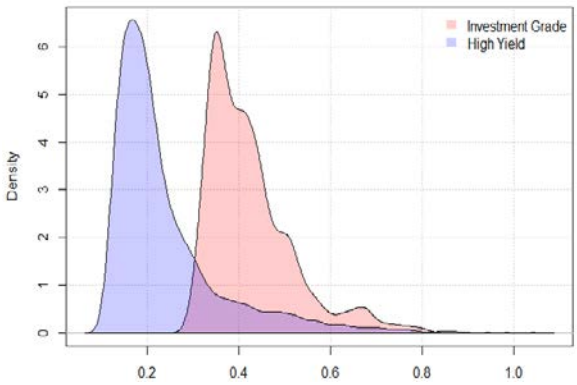

Panel B: Energy sector index

a). Downside VaR

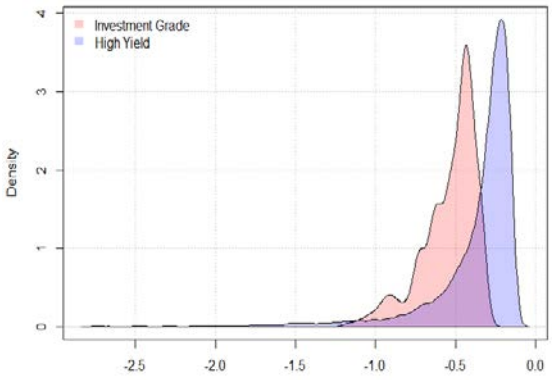

b). Upside VaR

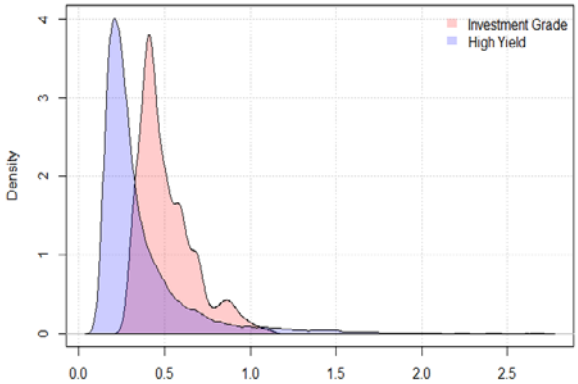

Notes: Downside and upside VaRs are calculated under the quantiles of 5% and 95%, respectively. See notes to Table A.2 for further details.

References:

Aloui, R., Hammoudeh, S., & Nguyen, D. K. (2013). A time-varying copula approach to oil and stock market dependence: The case of transition economies. Energy Economics, 39, 208-221.

Cherubini, U., Luciano, E., & Vecchiato, W. (2004). Copula methods in finance. John Wiley & Sons.

Christoffersen, P. F. (1998). Evaluating interval forecasts. *International economic review*, 841-862.

Dumitrescu, E. I., Hurlin, C., & Pham, V. (2012). Backtesting value-at-risk: from dynamic quantile to dynamic binary tests. *Finance*, 33(1), 79-112.

Engle, R. F., & Manganelli, S. (2004). CAViaR: Conditional autoregressive value at risk by regression quantiles. *Journal of Business & Economic Statistics*, *22*(4), 367-381.

Hollander, M., & Wolfe, D. A. (1973). Nonparametric statistical procedures. New York: Willey.

International Energy Agency (IEA) (2019a). Oil 2019 Analysis and forecast to 2024. Retrieved from: https://webstore.iea.org/download/summary/2446?fileName=English-Oil-2019-ES.pdf

International Energy Agency (IEA) (2019b). Gas 2019 Analysis and forecast to 2024. Retrieved from: https://www.iea.org/gas2019/

Uddin, G. S., Hernandez, J. A., Shahzad, S. J. H., & Hedström, A. (2018). Multivariate dependence and spillover effects across energy commodities and diversification potentials of carbon assets. Energy Economics, (2018), 35-46